Figures 1 and 2 show typical signal recovery performance. Figure 1(a) shows a distorted, 500 MHz, 5 mV rms fundamental sine wave (obtained by overdriving the oscillator) as photographed directly from the face of the sampling oscilloscope. Figure 1(b) is also taken from the sampling oscilloscope, now with 100 mV rms noise added. Figure 2 shows three successive traces from the digital oscilloscope showing the results of integrating for 2, 10, and 50 sec, respectively (reading upward). Note the comparative clarity after 50 sec of integration. Note also the preservation of the waveform (phase relationship of the signal harmonics), something difficult to do using simple RC integration unless extremely slow sweep speeds are used.

The 500 MHz frequency of the signals shown here should not be taken as an indication of the limit of the instruments bandwidth. We have measured the system's risetime to be faster than 40 psec (the limit of our equipment). The specifications for the sampling head indicate a 3 dB bandwidth of 14 GHz (i.e., a risetime of 25 psec). The system has shown itself to be easily capable of recovering a 100 psec risetime pulse reflected from a probe tip immersed in a turbulent (i.e., extremely noisy) plasma with sufficient accuracy to allow measuring the direct signal coupling between the probe and plasma. The signal level was 45 dB less than the noise level.

Figure 3 shows a block diagram of the uhf digital signal averager. The operation is almost self-explanatory. The time resolution is controlled by the time/div switch on the sampling oscilloscope. The sampling output of this oscilloscope is fed to the vertical input of the digital oscilloscope. The digital oscilloscope, in turn, controls the sweeping of both units in real time (as shown) and the signal integration time. The sweep should be fast enough to be flicker free, but slow enough to preserve digitizing accuracy. The integration time is, of course, dictated by the amount of noise present. However, at low integration times the human eye becomes an averager; for example, the signal in Fig. 2 is plainly visible to the eye (as a fixed skeleton about which the data points seem to move) with less than 2 sec of integration time. The effect of varying experimental parameters is thus visible immediately, even on a signal buried 40 dB in noise. As always when signal averaging is used, a trigger signal must be available either on the input waveform or from an external source synchronous with the signal of interest.

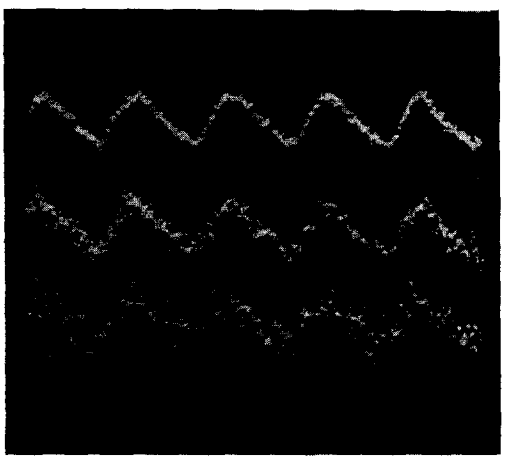

FIG. 2. Photographs of the signal in Fig. 1(b) after processing by the digital oscilloscope using 2, 10, and 50 sec of integration time successively (reading upward).

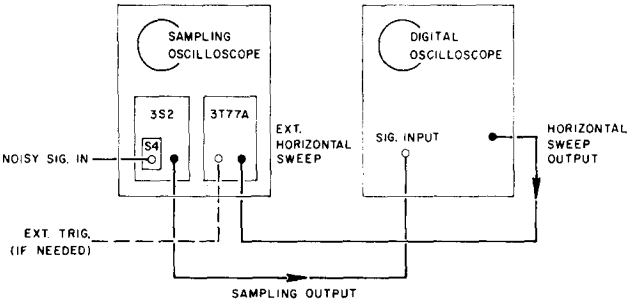

FIG. 3. Block diagram of a uhf digital signal averager obtained by combining a sampling oscilloscope and a digital signal averaging oscilloscope. Note that the wiring connections are all made through front panel terminals.

The author gratefully acknowledges the interest and suggestions of I. Alexeff, R. V. Neidigh, and W. D. Jones.

* Research sponsored by the U. S. Atomic Energy Commission undercontract with the Union Carbide Corp.

† Student guest, University of Iowa.

[1] For example, Hewlett-Packard, Northern Scientific, Fabri-Tek, and Digital Equipment Corp. digital signal averagers all have bandwidths of 50 kHz or less.

[2] P. Bletzinger, A. Garscadden, I. Alexeff, and W. D. Jones, J. Sci. Instrum. **42**, 358 (1965).

[3] Tektronix Instruction Manual for 3T77A sampling sweep, p. 2.

[4] E. J. Fulcomer and J. M. Nemchik, Rev. Sci. Instrum. **40**, 1638 (1969).

[5] I. Alexeff, R. Neidigh, and W. R. Wing, Int. J. Eng. Sci. **7**, 531 (1969).

[6] The equipment used here included a Northern 513 digital oscilloscope, a Tektronix 3T77A sampling sweep, a Tektronix 3S2 sampling unit, and an S4 sampling head (which has a 3 dB point of 14 GHz) all mounted in a Tektronix 564 main frame. Alternatively, a Tektronix 3T2 sampling sweep has been used when it was necessary to realize the full bandwidth of the S4 head.

A Coupled Photometer and Respirometer

A. P. JACOBSON

School of Public Health, The University of Michigan, Ann Arbor, Michigan 48104

(Received 15 December 1969; and in final form, 26 June 1970)

SOME radiobiological effects are transient. They occur during irradiation and recover rapidly thereafter. For example, bacterial luminescence is suppressed within seconds by x rays and recovers immediately.[1,2] Continuous monitoring is essential since lengthy analytical

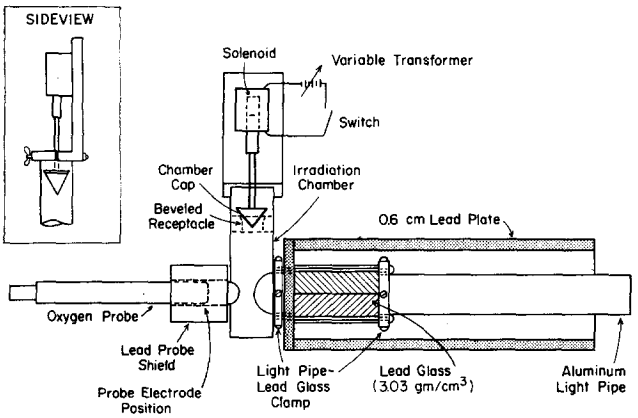

FIG. 1. Irradiation chamber assembly with shielded light pipe. Scale 0.22:1

methods will not detect these transient events. Studies aimed at the molecular mechanisms of these immediate and reversible radiation effects indicate the need to measure oxygen and bioluminescence simultaneously, since luminescence, respiration, and many radiation induced reactions require oxygen. A simple arrangement which allows such continuous measurements is described.

Special features of this apparatus are an aluminum irradiation chamber, a polarographic oxygen probe, and a "light pipe" of lead glass and aluminum (see Fig. 1). The aluminum chamber serves to couple the oxygen probe and light pipe and to contain the luminous sample. For radiation studies, the chamber is positioned in the beam of an x-ray generator.[3]

Although glass and plastic vessels do not affect biological systems, they fluoresce intensely during irradiation and are unacceptable as material for the irradiation chamber. Aluminum was chosen for this application because it fluoresces little during irradiation, is stronger than glass or plastic, and does not inhibit bioluminescence.

The oxygen probe, a galvanic membrane electrode system based on a design by Mancy and Westgarth[4] and similar to those described by Clark,[5] produces current proportional to the partial pressure of oxygen at the electrodes. Calibration was done by an Alsterberg modification of the Winkler method of determining dissolved oxygen in complex media.[6] Probe current was linearly proportional to oxygen concentration up to 33 mg oxygen/liter, the highest tested.

The chamber cap is an aluminum cone fitted to a beveled receptacle which seals the chamber and prevents entrapment of air. This ensures accurate determinations of dissolved oxygen without replacement by air trapped in the sample.

The light pipe is a polished aluminum tube. Fluorescence and scattered x rays from the sample are attenuated strongly by the lead glass while luminescence is not.[7] The distal end of the light pipe shown in Fig. 1 fits into a lead shielded photomultiplier tube (PMT) housing. The design of this housing can be varied but must provide shielding against ambient light, scattered x rays, and magnetic disturbances. The light path is controlled with a solenoid driven shutter between the light pipe and PMT.

Signals from the oxygen probe and PMT were amplified with picoammeters.[8] Oxygen probe signals ranged from 1 to 10 μA, those of the PMT from 10 to 100 nA. The outputs of both picoammeters were coupled to a dual channel strip-chart recorder[9] driven at 1 mm/sec. The time constant for the photometer measuring circuit was 0.5 sec for all current ranges used.

Experiments begin when a bioluminescent sample is placed in the irradiation chamber and warmed by an air bath to 23.0±0.3°C. The chamber is sealed by lowering its cap. The light path is opened. Next, the sample is exposed to x rays.[3] Luminescence and dissolved oxygen are measured continuously and recorded. Three minutes after exposure, the light path is closed and the sample removed.

Figure 2 shows the significant events of an experiment. Although a lead shield protects the electrode from direct x irradiation, complete shielding is difficult because of

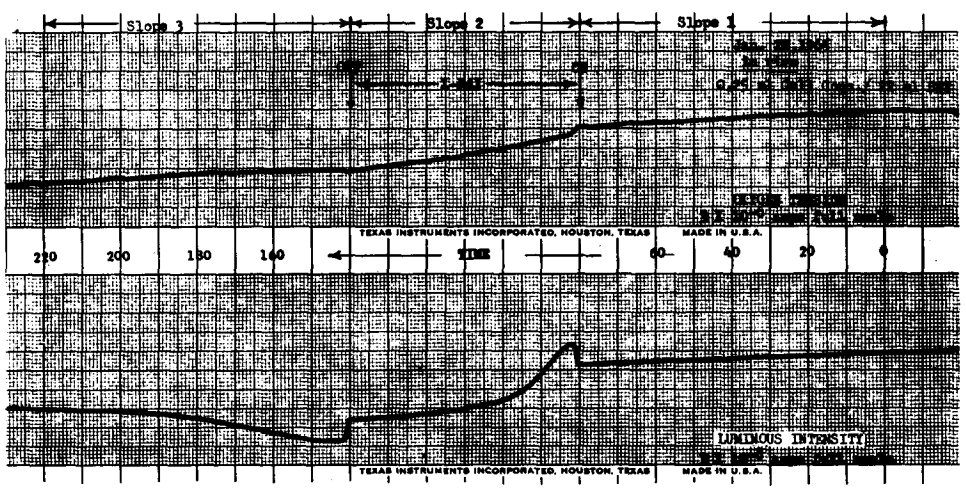

FIG. 2. Respiring cells consume oxygen inside the closed chamber; the resulting decrease of dissolved oxygen is recorded in the upper tracing. After a determination of the normal rate of oxygen uptake by cells, the behavior of both luminescence and oxygen uptake during exposure is recorded. Data are recorded after an exposure for a period sufficiently long to ensure that all important changes have been observed. The lower portion of the chart records the phototube signal for the same time period. The units are arbitrary and usually expressed as amperes $\times 10^{-8}$. The rise of phototube current at the onset of exposure is a radiation induced artifact, is constant throughout the irradiation, and is subtracted for analysis of the curves.

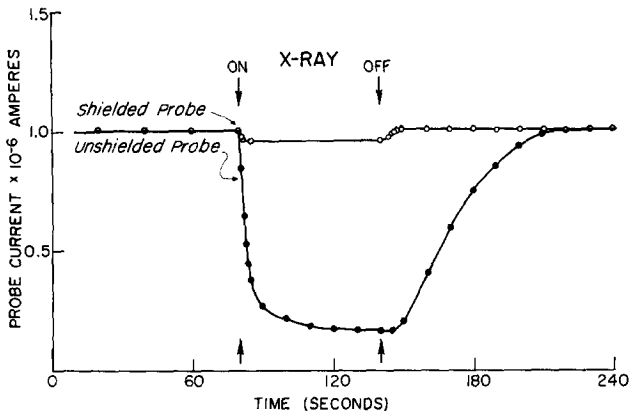

FIG. 3. A comparison of the effect of x rays on oxygen probe current between shielded and unshielded probes. The shield consists of lead sheet coiled to a thickness of 1 cm. The dose rate was 100 rad/sec.[3] This response is identical in distilled water and solutions of heat killed cells.

scattered x rays. This radiation effect on the oxygen electrode is apparent in Fig. 2. Figure 3 compares shielded and unshielded electrode response in x-irradiated, continuously aerated distilled water. The radiation effect on shielded electrodes is constant under these conditions and disappears completely within 10 sec after irradiation. This radiation effect on the probe is identical in distilled water and in suspensions of heat killed bacteria.[9]

Radiation induced fluorescence is the most serious problem with the photometer. Lead glass and the aluminum light pipe substantially reduce this artifact but do not eliminate it. The rise of PMT current at the onset of irradiation in Fig. 2 is due to radiation induced fluorescence and scattered x rays. Figure 4 shows that the artifact is small and constant for nonluminescent samples of heat killed cells. The dotted line of Fig. 4 shows the behavior of luminescence after this artifact is subtracted.

The reversible suppression of luminescence has been shown to be a metabolic response to x rays that can be modified by various sample treatments. The behavior of

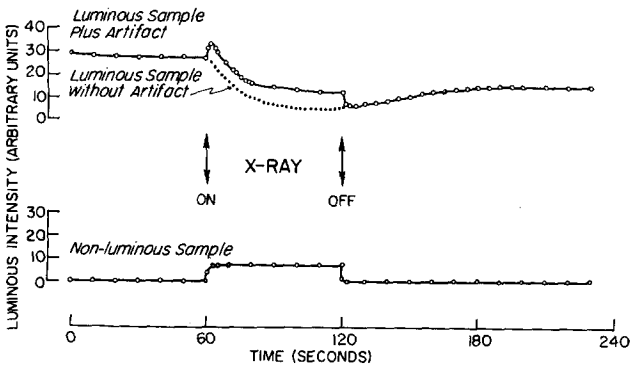

FIG. 4. Photometer response to luminous samples during irradiation includes luminescence, x-ray-induced fluorescence, and scattered x rays (upper curve). The magnitude of phototube current due to x rays and fluorescence is measured in nonluminous samples (lower curve) and subtracted from the total response curve. The net effect shows the biological response to irradiation.

TABLE I. Reliability data for five features of luminescence curves before, during, and after irradiation. The range, mean, and standard deviation are presented for a set of 10 typical luminous cell samples.

Item	Units	Range	Mean	Standard deviation
Initial luminescence prior to exposure	$A\times10^{-8}$	1.28 -1.10	1.16	±0.07
Maximum rate of suppression during exposure	$A/sec\times10^{-8}$	0.057–0.048	0.052	±0.003
Total suppression due to x rays	$A\times10^{-8}$	0.94–0.75	0.78	±0.05
Maximum rate of recovery	$A/sec\times10^{-8}$	0.933–0.027	0.031	±0.002
Final luminescence after exposure	$A\times10^{-8}$	1.13–0.96	1.01	±0.06

this phenomenon is predictable and reproducible within acceptable limits. Table I provides some data reliability figures. The range and mean for a given quality of luminescence are listed with the standard deviation as an estimate of the limits of error for a typical set of 10 cell samples.

The average standard error for a series of consecutive determinations of the rate of oxygen uptake by cells is approximately 5% ($\bar{x}=0.435\pm0.020$ mg O_2 10^{-3}/liter·sec). The estimate for errors in chemical oxygen determinations for probe calibration is largely due to errors of titration with sodium thiosulfate.[6] Each milliliter of sodium thiosulfate titrant used in the determination is equivalent to 1 mg/liter dissolved oxygen in solution. The standard deviation of such determinations is typically 0.05 ml of sodium thiosulfate.

[1] C. H. Burns, A. P. Jacobson, and G. H. Whipple, Radiation Res. 24, 494 (1965).
[2] O. Hug, and I. Wolf in *Progress in Radiobiology*, Proc. 4th Intern. Conf. Radiobiol., Cambridge, England (1956).
[3] G. E. Maxitron 300 x-ray generator operated at 300 kV p, 20 mA, 4.75 mm beryllium window, *HVL* (half-value layer) = 0.75 cm aluminum, 100 rad/sec.
[4] K. H. Mancy and W. C. Westgarth, J. Water Pollut. Control Fed. 34, 1037 (1962).
[5] L. C. Clark, Jr. Trans. Amer. Soc. Artificial Internal Organs 2, 41 (1956).
[6] *Standard Methods for the Examination of Water, Sewage, and Industrial Wastes* (American Public Health Association, New York, 1965), 12th ed.
[7] A. P. Jacobson (unpublished).
[8] Keithley Instruments, Inc., Cleveland, Ohio, model 410 micromicroammeter.
[9] Texas Instruments, Inc., Houston, Texas, model P2CAN two channel recorder.

Sphere Grinder Improvement

P. B. CRANDALL

Science Center, North American Rockwell Corporation, Thousand Oaks, California 91360

(Received 27 July 1970; and in final form, 17 August 1970)

SCHUYFF and Hulscher[1] describe a sphere grinder that has proven successful in the making of small spheres of fragile crystals. Using their basic idea, the design of the